Journal of Sound and Vibration (1999) **228**(3), 651–682
Article No. jsvi.1999.2440, available online at http://www.idealibrary.com on IDEAL®

A MECHANICAL FILTER CONCEPT FOR CONTROL OF NON-LINEAR CRANE-LOAD OSCILLATIONS

B. Balachandran and Y.-Y. Li

Department of Mechanical Engineering, University of Maryland, College Park, MD 20742-3035, *U.S.A.*

and

C.-C. Fang

Department of Electrical Engineering, University of Maryland, College Park, MD 20742-3035, *U.S.A.*

(*Received* 14 *August* 1998, *and in final form* 8 *June* 1999)

In this article, results obtained through analytical and numerical investigations into the control of planar, large-amplitude crane-load oscillations are presented. A novel concept called a *mechanical filter* is proposed and described. In the context of ship crane-load oscillations, this concept is implemented on the basis of the premise that by controlling the pivot point about which the load oscillates, one can effectively suppress crane-load oscillations. Ship-roll-induced load oscillations are considered and a "mechanical filter" is introduced at the pivot to control these oscillations. The pivot is constrained to follow a circular track in the considered filter. The governing non-linear dynamical systems for the cases with and without the filter are presented. Transfer functions are determined for the linearized dynamical systems and the filter performance characteristics are discussed. The non-linear dynamics of the systems with and without the filter is studied with respect to quasi-static variation of different scalar control parameters. Static feedback laws for actively controlling the pivot motions are also considered and the dynamics in the controlled cases is compared with the dynamics in the corresponding uncontrolled cases. It is shown that the presence of the filter helps in eliminating some of the subcritical bifurcations that may arise in the crane-load response during periodic ship-roll excitations. The presence of feedback control also allows us to effectively suppress transient crane-load oscillations.

1. INTRODUCTION

Crane ships are often used at sea transfer to cargo from large vessels to light vessels, which are used to transport the cargo to shore. During the transfer process, wave-induced motions of the considered crane vessel can result in substantial, undesired oscillations of the crane load [1–3]. Instability of crane-load motions during harmonic forcing has been investigated by Patel *et al.* [1] by using a model with a parametric excitation term. In the studies of McCormick and Witz [2] and

0022-460X/99/480651 + 32 $30.00/0

Witz [3], time-domain simulations were carried out to examine the instabilities due to parametric excitations produced by random sea states. Chin and Nayfeh [4] used perturbation analysis and numerical simulations to investigate a weakly non-linear model of a ship–crane system. They paid attention to parametric instabilities that arise when the crane load is allowed to swing in a three-dimensional space.

Many studies on dynamics and control of crane-load motions have been reported in the literature for cranes operating on fixed platforms. These studies can be classified under one of the following categories: (1) overhead gantry cranes and (2) rotary cranes. Overhead gantry cranes have been treated in the efforts of Auernig and Troger [5], Moustafa and Ebeid [6], d'Andréa-Novel and Levine [7], Ebeid *et al.* [8], and Fleiss *et al.* [9]. Rotary cranes have been considered by Sakawa and Nakazumi [10], Souissi and Koivo [11], and Parker *et al.* [12]. Although various aspects related to cargo handling and load transfer have been addressed in the above-mentioned efforts, these efforts primarily address crane-load oscillations that arise due to transient disturbances. For a crane operating on a floating platform such as a ship vessel, it is important to consider large-amplitude, crane-load motions caused by persistent disturbances as well as transient disturbances.

With the long-term objective of developing a scheme for controlling large-amplitude crane-load oscillations on a floating platform, a novel concept called a *mechanical filter* is proposed and explored here. In a broad sense, the terminology of *mechanical filter* is used here to mean a mechanical construction, a device or a set of devices whose introduction into a system will lead to suppression or elimination of undesired dynamics in the considered system. The attributes of the proposed mechanical filter include the following: (1) the filter is constructed by using mechanical devices, (2) its performance depends on the characteristics of the system into which it is introduced, (3) its performance in certain regions of the state-control space (i.e., space of state variables and control parameters) may be characterized by transfer functions while the performance in other regions of the state-control space may be characterized by using non-linear analysis and tools such as bifurcation diagrams, and (4) the elements of the filter can include passive as well as active devices. Here, it is intended to use this concept for suppressing or eliminating undesired crane-load motions. The concept of a mechanical filter is different from the concepts of acoustic filters and electric filters that are used in the literature. The terminology of *acoustic filters* is used to describe mechanical devices that are used to allow for passage of acoustic signals with a certain frequency content, and the terminology of *electric filters* is used to describe electronic devices that are used to allow for passage of signals with the desired frequency content [13]. The performance of acoustic filters is typically dependent upon the acoustic system into which they are inserted, the dimensions and characteristics of the mechanical device, and the wavelengths involved. On the other hand, the performance of electric filters is typically dependent upon the electrical characteristics of the electronic components involved and the filter performance is characterized by transfer functions for filters idealized as linear systems. Furthermore, by and large, the design of acoustic and electric filters is carried out by using passive devices.

In the recent study of Iwasaki *et al.* [14], the addition of a "secondary" mass to a primary floating crane system was considered and active control of motions of the "secondary" mass was explored for attenuating crane-load oscillations. Here, the proposed filter is meant to be used for suppression of "large" crane-load oscillations. The proposed filter may be construed as a vibration absorber designed for a mechanical system, in which traditionally a "secondary" system called the absorber is added to absorb the oscillations of the "primary" system [15]. In the past, such absorbers have been designed for linear and non-linear mechanical systems. In the non-linear systems considered in related previous studies [16–22], the components of either the "secondary" system or the "primary" system alone have non-linear characteristics. Furthermore, typically, in the analysis and related numerical simulations, "weakly" non-linear systems are considered and attention is paid to the response characteristics in the frequency domain to highlight the suppression of motions in a certain frequency bandwidth. There are several features that distinguish the current study from the earlier studies on absorbers in non-linear systems; these features include the following: (1) use of the "secondary" system or the filter to suppress subcritical bifurcations and related "large" oscillations, (2) use of the filter to shift bifurcation points out of the considered parameter windows, (3) consideration of response characteristics with respect to control parameters such as excitation frequency and excitation amplitude, and (4) use of active/passive control strategies in the filter design. Here, the words "mechanical filter" are used in preference to the words "vibration absorber" because the filter design is broader in scope than the design of a conventional "vibration absorber", which is primarily designed to attenuate response characteristics in the frequency domain.

The present article is an extended form of the work reported by Balachandran and Li [23]. New results obtained since that work was reported are also included in the current article. The rest of this article is organized as follows. In section 2, the filter concept proposed for suppression of crane-load oscillations is presented along with the dynamical systems for the cases with and without the filter. For "small" crane-load oscillations, linear analyses are carried out and transfer functions are obtained to characterize the filter performance. In section 3, for "large" crane-load oscillations, non-linear analyses are carried out to characterize the filter and the results are examined in the state-control space by using bifurcation diagrams. Comparisons between the behavior of the system with the passive filter and the behavior of the system with the active filter are also made in this section. Finally, concluding remarks are provided to close this article.

2. FILTER CONCEPT AND DYNAMICAL SYSTEMS

In this section, the "mechanical filter" proposed for controlling planar crane-load oscillations is presented and the dynamical systems for cases with and without the filter are provided. These dynamical systems have been derived by using the Lagrangian for the corresponding systems. (The steps leading to the governing equations from the Lagrangian are not shown here for brevity). The different

excitations considered and the form of feedback control law examined are also provided in this section.

2.1. MECHANICAL FILTER

In Figure 1, side views of a conventional crane configuration and a modified crane configuration are illustrated along with an enlarged insert of the proposed filter. The longitudinal axis of the vessel about which the roll oscillations take place is normal to the considered side view. For simplicity, only planar motions of the cargo load that may arise as a result of ship-roll motions are considered here. The boom orientation in the vertical plane is specified by the angle ϕ in Figure 1. Furthermore, the boom configuration is assumed to be rigid in the analysis.

Based on the premise that the crane-load oscillations are to be controlled by controlling the pivot point about which the load oscillates, at the initial stage of this work, a mechanical device was sought to reduce the effective excitation felt by the crane load due to the ship motions. This led us to choose a mechanical filter, which was essentially a smooth, circular track with elastic restraints for the pivot. Although actuators are not shown in the figure, it is assumed that the pivot can be actuated by a control input u. The filter can be thought of as being passive without the actuators, and with the actuators, the filter has both passive and active attributes. For a system, such as a ship crane vessel, the actuations required for controlling the crane-load motions can be "large" and usually one is limited by the magnitude of actuation available for controlling the motions. Hence, often, a (hybrid) control scheme with active and passive elements is required for

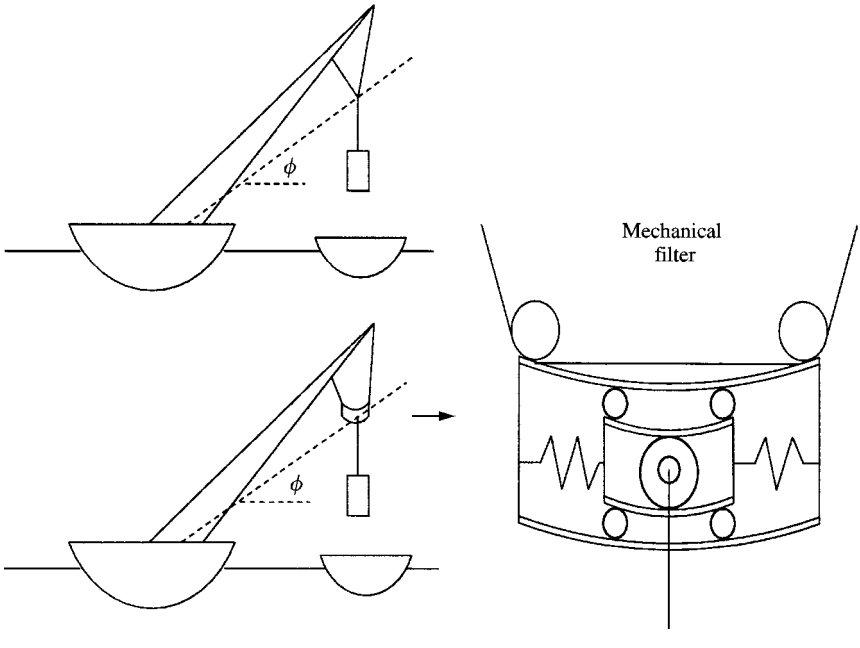

Figure 1. Illustrations of crane configuration with and without the filter.

controlling crane-load motions. This consideration has been taken into account in the construction of the filter.

2.2. DYNAMICAL SYSTEMS FOR CASES WITH AND WITHOUT FILTER

The roll oscillations of the ship-crane vessel translate to an excitation with horizontal and vertical components at the crane pivot. In the geometries illustrated in Figures 2 and 3, the excitation components along he X- and Y-axis are expressed by x_e and y_e, respectively. The mass of the crane load is represented by m_1 and the length of the cable is expressed by R_1. The cable is assumed to be inextensional and massless, and the angle θ is used to describe the motions of m_1. For this planar pendulum, after inclusion of damping, the governing equation obtained takes the form

$$m_1 R_1^2 \ddot{\theta} + m_1 R_1(-\ddot{x}_e \sin\theta + \ddot{y}_e \cos\theta) + m_1 g R_1 \sin\theta + c_\theta \dot{\theta} = 0. \tag{1}$$

Equation (1) will be referred to as the dynamical system without the filter for purposes of further discussion in this article. From the form of this excitation, the presence of both parametric and external excitation terms can be discerned.

In Figure 3, the co-ordinates used to describe the motion of the system with the filter are illustrated. The mass of the pivot is represented by m_2, the stiffness of the spring on each side of the pivot is represented by k, and the dimensions of this mass are assumed to be "small" with respect to the pivot radius R_2. On this track, the motion of mass m_2 is constrained to follow the equation

$$(x + R_2)^2 + y^2 = R_2^2. \tag{2}$$

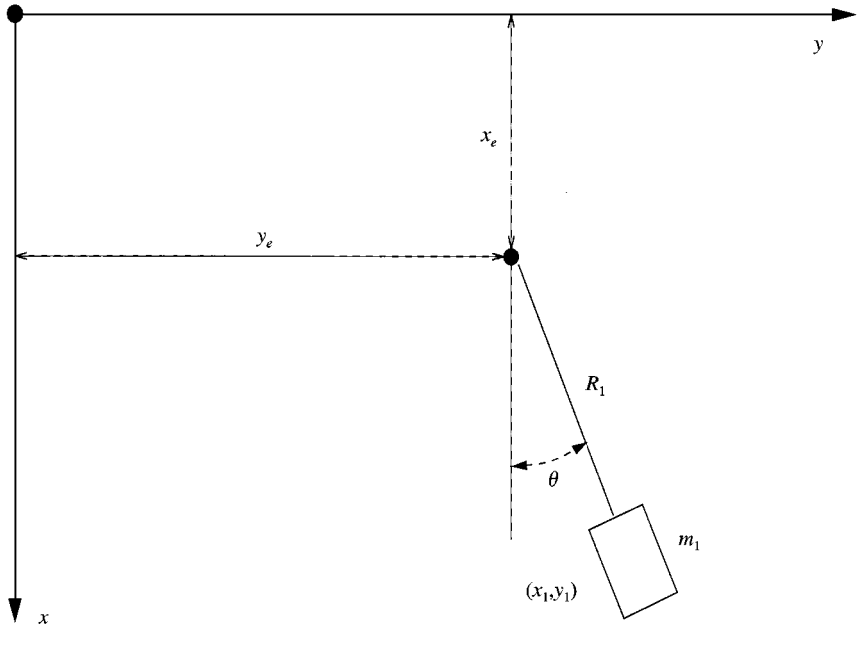

Figure 2. Geometry for planar system without the filter.

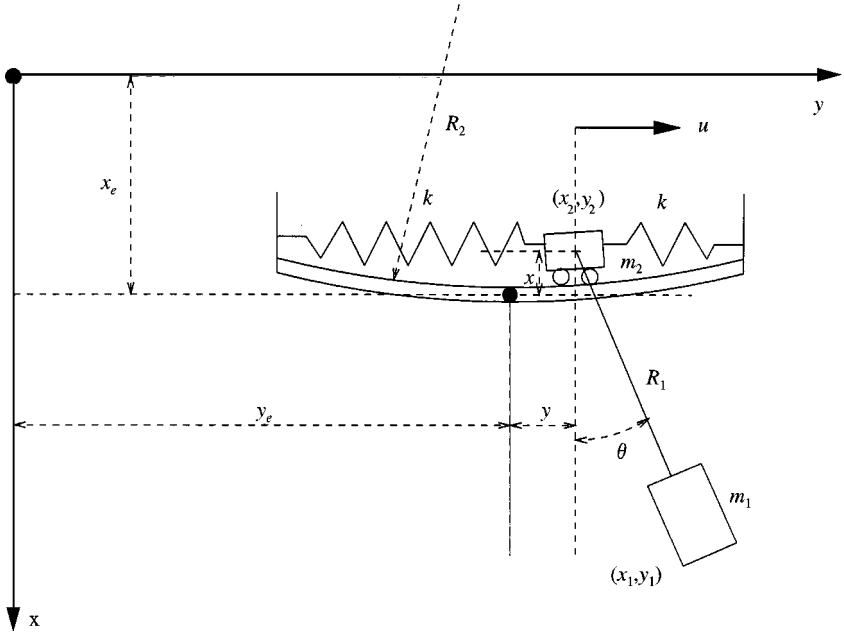

Figure 3. Geometry for planar system with the filter.

From equation (2), one arrives at

$$x + R_2 = \sqrt{R_2^2 - y^2} = R_2\sqrt{1 - \frac{y^2}{R_2^2}}, \tag{3}$$

which when assumed that $|y/R_2| \ll 1$ leads to

$$x + R_2 = R_2\left[1 + \frac{1}{2}\left(-\frac{y^2}{R_2^2}\right) - \frac{1}{2\cdot 4}\left(-\frac{y^2}{R_2^2}\right)^2 + \cdots\right]. \tag{4}$$

Retaining only the first few terms in equation (4), the vertical displacement x of mass m_2 can be related to the horizontal displacement y of mass m_2 through the relation

$$x = -\frac{y^2}{2R_2} - \frac{y^4}{8R_2^3} + \cdots. \tag{5}$$

In arriving at equation (5) from equation (2), the circular track over which the pivot is constrained to move has been replaced by a parabolic track. In the numerical studies reported in sections 3 and 4, the results are presented for $R_2 = 10$, 50 m, and higher values of R_2. Through numerical work, it has been ascertained that for $R_2 = 10$ and 50 m, equation (5) is a "good" approximation for equation (2) as long as $|y| < 7{\cdot}5$ m and < 35 m, respectively. As R_2 is increased further, there is a rapid increase in the range of y over which equation (5) is a "good" approximation for equation (2).

After inclusion of damping, the governing equations for the planar system with the filter are determined to be of the form

$$m_1 R_1^2 \ddot{\theta} + m_1 R_1 \left[-\ddot{x}_e \sin\theta + (\ddot{y} + \ddot{y}_e)\cos\theta + \left(\frac{y}{R_2} + \frac{y^3}{2R_2^3}\right)\sin\theta\ddot{y} + \left(\frac{1}{R_2} + \frac{3y^2}{2R_2^3}\right)\sin\theta\dot{y}^2 \right] + m_1 g R_1 \sin\theta + c_\theta \dot{\theta} = 0, \tag{6}$$

$$m_1 R_1^2 \ddot{\theta}\left[\left(\frac{y}{R_2} + \frac{y^3}{2R_2^3}\right)\sin\theta + \cos\theta\right] + m_1 R_1 \dot{\theta}^2 \left[\left(\frac{y}{R_2} + \frac{y^3}{2R_2^3}\right)\cos\theta - \sin\theta\right] - (m_1 + m_2)\left[\frac{y}{R_2} + \frac{y^3}{2R_2^3}\right]\ddot{x}_e - (m_1 + m_2)\left[1 + \left(\frac{y}{R_2} + \frac{y^3}{2R_2^3}\right)^2\right]\ddot{y} + (m_1 + m_2)\ddot{y}_e \rightarrow (m_1 + m_2) g \left(\frac{y}{R_2} + \frac{y^3}{2R_2^3}\right) + (m_1 + m_2)\left(\frac{y}{R_2} + \frac{y^3}{2R_2^3}\right)\left(\frac{1}{R_2} + \frac{3y^3}{2R_2^3}\right)\dot{y}^2 + c_y \dot{y} + 2ky = u. \tag{7}$$

In the rest of this article, equations (6) and (7) will be collectively referred to as the dynamical system with the filter. Again, the presence of both parametric and external excitation terms can be noticed in the dynamical system with the filter. The introduction of the filter leads to new non-linear terms in the governing equations. The strengths of these terms depend on the pivot track radius R_2. As the pivot track becomes flat, R_2 becomes large and the magnitudes of the corresponding non-linear terms in equations (6) and (7) become smaller. The limit $R_2 \rightarrow \infty$ corresponds to the completely flat track case. In this case, any position of the pivot on the track will correspond to an equilibrium position. However, for a track with a finite radius (i.e., $R_2 \neq 0$), the bottom of the track will correspond to the equilibrium position of the pivot. Furthermore, comparing the dynamical systems with and without the filter, one can make the following observations: (1) the equilibrium positions $(\theta, \dot{\theta}) = (0, 0)$ and $(\theta, \dot{\theta}) = (\pi, 0)$ of the crane load m_1 are preserved after introduction of the filter, (2) the filter geometry is such that $(y, \dot{y}) = (0, 0)$ is the equilibrium position for the pivot m_2, and (3) the two-dimensional dynamical system without the filter is "embedded" in the four-dimensional dynamical system with the filter.

2.3. EXCITATIONS DUE TO SHIP-ROLL MOTIONS

The excitation at the pivot of the planar system due to the roll motions of the vessel is considered to be either harmonic or periodic. In the harmonic case, the

excitation components x_e and y_e are given by

$$x_e = (F \sin \omega t) \cos \phi, \quad y_e = (F \sin \omega t) \sin \phi. \tag{8}$$

where F is the excitation amplitude and ω is the excitation frequency. In the periodic case, the excitation components are given by

$$x_e = F(\sin \omega t + \tfrac{1}{4} \sin 2\omega t + \tfrac{1}{9} \sin 3\omega \mathrm{t}) \cos \phi,$$

$$y_e = F(\sin \omega t + \tfrac{1}{4} \sin 2\omega t + \tfrac{1}{9} \sin 3\omega \mathrm{t}) \sin \phi. \tag{9}$$

It is noted that other forms of periodic excitations could have been chosen, but here an arbitrary form was chosen to primarily illustrate the effectiveness of the filter. For the numerical results reported in section 4, the boom orientation angle $\phi = 30^\circ$, the excitation amplitude F is varied in the range of 0·0–5·0 m, and the excitation frequency is varied in the range of 0·47–2·00 rad/s.

2.4. CONTROL LAW

In the dynamical system comprising equations (6) and (7), when the control input $u = 0$, the corresponding cases are referred to as "passive control" or "passive filter" cases. If it otherwise, the corresponding cases are referred to as "active control" or "active filter" cases. The control law considered here is of the form

$$u = m_1(A \sin \theta + B\dot{y} + Cy). \tag{10}$$

The feedback law (10) is called *static feedback* following the description provided by Nayfeh and Balachandran [24]. Physically, the first term in equation (10) represents an input component provided to the pivot in proportion to the pendulum swing. The second term in equation (10) represents an input component that can be used to enhance the dissipation for the pivot motion, and hence, the dissipation in the overall system. The third term in equation (10) represents an input component that can be used to alter the stiffness characteristics related to the pivot motions.

3. LINEAR ANALYSES

The dynamical systems presented in the previous section are investigated in this section through linear analyses. In the analyses, the oscillations about the vertical position of the planar pendulum (i.e., $(\theta, \dot{\theta}) = (0, 0)$) are considered. The initial conditions are assumed to b trivial in all cases and the transfer functions are determined to characterize the performance of the filter for "small" oscillations about the trivial equilibrium position. It is to be noted that the analyses provided in this section will be valid for all excitation amplitudes only if the considered system's behavior is linear. However, as shown in the next section, the system's behavior is

not linear, and hence, the discussion provided here is valid only over a certain window of the considered parameters.

3.1. SYSTEM WITHOUT FILTER

For "small" oscillations of the planar pendulum about the trivial equilibrium position, (equation (1) can be linearized to obtain

$$m_1 R_1^2 \ddot{\theta} + m_1 R_1 \ddot{y}_e + m_1 g R_1 \theta + c_\theta \dot{\theta} = 0. \tag{11}$$

It is to be noted that in equation (11), the term corresponding to y_e is the excitation input. Assuming that the initial conditions are trivial and carrying out the Laplace transforms of different terms in equation (11) leads us to

$$m_1 R_1^2 s^2 \theta(s) + m_1 R_1 s^2 y_e(s) + m_1 g R_1 \theta(s) + c_\theta s \theta(s) = 0. \tag{12}$$

Then, the transfer function between the crane-load displacement treated as output and the horizontal excitation component treated as input takes the form

$$T(s) = \frac{\theta(s)}{y_e(s)} = \frac{-s^2}{R_1 s^2 + (c_\theta / m_1 R_1) s + g}. \tag{13}$$

3.2. SYSTEM WITH FILTER

For "small" oscillations of the system about the trivial equilibrium position $(\theta, \dot{\theta}, y, y) = (0, 0, 0, 0)$, equations (6) and (7) can be linearized to respectively obtain

$$m_1 R_1^2 \ddot{\theta} + m_1 R_1 (\ddot{y} + \ddot{y}_e) + m_1 g R_1 \theta + c_\theta \dot{\theta} = 0, \tag{14}$$

$$m_1 R_1^2 \ddot{\theta} + (m_1 + m_2)\ddot{y} + (m_1 + m_2)\ddot{y}_e + (m_1 + m_2)\, g \frac{y}{R_2} + c_y \dot{y} + 2ky$$

$$= m_1 (A\theta + B\dot{y} + Cy). \tag{15}$$

Equation (10) has been considered in arriving at equation (15). Again, assuming that the initial conditions are trivial and executing the Laplace transforms of different terms in equations (14) and (15) leads us to

$$m_1 R_1^2 s^2 \theta(s) + m_1 R_1 [s^2 y(s) + s^2 y_e(s)] + m_1 g R_1 \theta(s) + c_\theta s \theta(s) = 0, \tag{16}$$

$$m_1 R_1^2 s^2 \theta(s) + (m_1 + m_2) s^2 y(s) + (m_1 + m_2) s^2 y_e(s) + (m_1 + m_2)\, g \frac{y(s)}{R_2}$$

$$+ c_y s y(s) + 2k y(s) = m_1 [A\theta(s) + Bsy(s) + Cy(s)]. \tag{17}$$

Based on equations (16) and (17), for the passive filter case [i.e., $A = B = C = 0$ in equation (17)], the transfer function between the crane-load displacement output and the horizontal excitation input is given by

$$T(s) = \frac{\theta(s)}{y_e(s)} = \left[\frac{c_y}{m_1}s + \frac{2k}{m_1} + \left(1 + \frac{m_2}{m_1}\right)\frac{g}{R_2}\right]s^2 \Bigg/ \left\{R_1 s^4 - \left(R_1 s^2 + \frac{c_\theta}{m_1 R_1}s + g\right)\left[\left(1 + \frac{m_2}{m_1}\right)s^2 + \frac{c_y}{m_1}s + \frac{2k}{m_1} + \left(1 + \frac{m_2}{m_1}\right)\frac{g}{R_2}\right]\right\}. \tag{18}$$

When one compares equation (18) with equation (13), it s clear that the introduction of the passive filter introduces two additional poles and one additional zero in the transfer function. These changes affect the performance of the system, as illustrated by the results provided in the next subsection. The transfer function between the pivot displacement output and the horizontal excitation input is given by

$$T(s) = \frac{y(s)}{y_e(s)} = \left[\left(1 + \frac{m_2}{m_1}\right)s^2\left(R_1 s^2 + \frac{c_\theta}{m_1 R_1}s + g\right) - R_1 s^4\right] \Bigg/ \left\{\left(R_1 s^4 - \left(R_1 s^2 + \frac{c_\theta}{m_1 R_1}s + g\right)\left[\left(1 + \frac{m_2}{m_1}\right)s^2 + \frac{c_y}{m_1}s + \frac{2k}{m_1} + \left(1 + \frac{m_2}{m_1}\right)\frac{g}{R_2}\right]\right)\right\}. \tag{19}$$

For the active filter case, the transfer function between the crane load displacement output and the horizontal excitation input is given by

$$T(s) = \frac{\theta(s)}{y_e(s)} = \left[\left(\frac{c_y}{m_1} - B\right)s + \frac{2k}{m_1} + \left(1 + \frac{m_2}{m_1}\right)\frac{g}{R_2} - C\right]s^2 \Bigg/ \left\{(R_1 s^4 - A)s^2 - \left(R_1 s^2 + \frac{c_\theta}{m_1 R_1}s + g\right)\left[\left(1 + \frac{m_2}{m_1}\right)s^2 + \left(\frac{c_y}{m_1} - B\right)s + \frac{2k}{m_1} + \left(1 + \frac{m_2}{m_1}\right)\frac{g}{R_2} - C\right]\right\}. \tag{20}$$

When one compares equation (20) with equation (13), the introduction of an active filter introduces one additional zero and two additional poles in the transfer function. On comparing the transfer functions for the passive and active filter cases

[i.e., equations (18) and (20)], it is evident that the system with the active filter has the same number of poles and zeros as the system with the passive filter. However, the feedback action shifts the locations of zeros and the poles. The effects of these changes on the performance of the system are discernible in the results provided in the next subsection. Here, the transfer function between the pivot displacement output and the horizontal excitation input is given by

$$T(s) = \frac{y(s)}{y_e(s)} = \left[\left(1 + \frac{m_2}{m_1}\right)s^2\left(R_1 s^2 + \frac{c_\theta}{m_1 R_1}\, s + g\right) - (R_1 s^2 - A)s^2\right] \Bigg/ \left\{(R_1 s^2 - A)s^2 - \left(R_1 s^2 + \frac{c_\theta}{m_1 R_1}\, s + g\right)\left[\left(1 + \frac{m_2}{m_1}\right)s^2 + \frac{c_y}{m_1}\, s + \frac{2k}{m_1} + \left(1 + \frac{m_2}{m_1}\right)\frac{g}{R_2} - Bs - C\right]\right\}. \tag{21}$$

Again, when one compares equation (21) with equation (19), one can see the differences in the locations of the poles and zeros between the passive and active filter cases.

3.3. NUMERICAL RESULTS

Numerical results obtained by using equations (13), (18), (19), (20), and (21) are illustrated in Figures 4–9. In each figure, the magnitude of the transfer function in decibels is shown on the y-axis (vertical axis) and the independent variable (i.e., the frequency ω) is shown on the x-axis (horizontal axis). The following parameter values are used in all of the cases where the filter is considered: (1) $\zeta_\theta = c_\theta/(m_1 R_1) = 0{\cdot}02$, (2) $\zeta_y = c_y/m_1 = 0{\cdot}0$, (3) $R_2 = 50$ m, (4) $k/m_1 = 0{\cdot}1$ units, and (5) $m_2/m_1 = 0{\cdot}01$. The numerical values for the different parameters have been primarily chosen to illustrate the performance characteristics of the mechanical filter, and as such, in the current work, no efforts have been made to design an optimal filter for a specific ship–crane vessel. Although cases with $\zeta_y = 0{\cdot}05$ have been considered, the corresponding results are not included here because they are qualitatively similar to those obtained for the cases with $\zeta_y = 0{\cdot}0$. In addition, the pivot motions are damped through velocity feedback in the active filter cases. Three different active filter cases are considered, and the parameter values in each case are provided in the discussion below.

In Figure 4, the magnitudes of the transfer functions are plotted for the following three cases: (1) system without filter, (2) system with passive filter [i.e., $u = 0$ in equation (7)], and (3) system with active filter. For the last case, the parameter values used in computing the control input are the following: (1) $A = 96{\cdot}2361$, (2) $B = -0{\cdot}5$, and (3) $C = 0{\cdot}0$. The response curves for the cases without the filter and with the passive filter qualitatively resemble those obtained respectively for a single-degree-of-freedom spring-mass–damper system and a two-degree-of—freedom system obtained by the addition of a vibration absorber [15]. Through

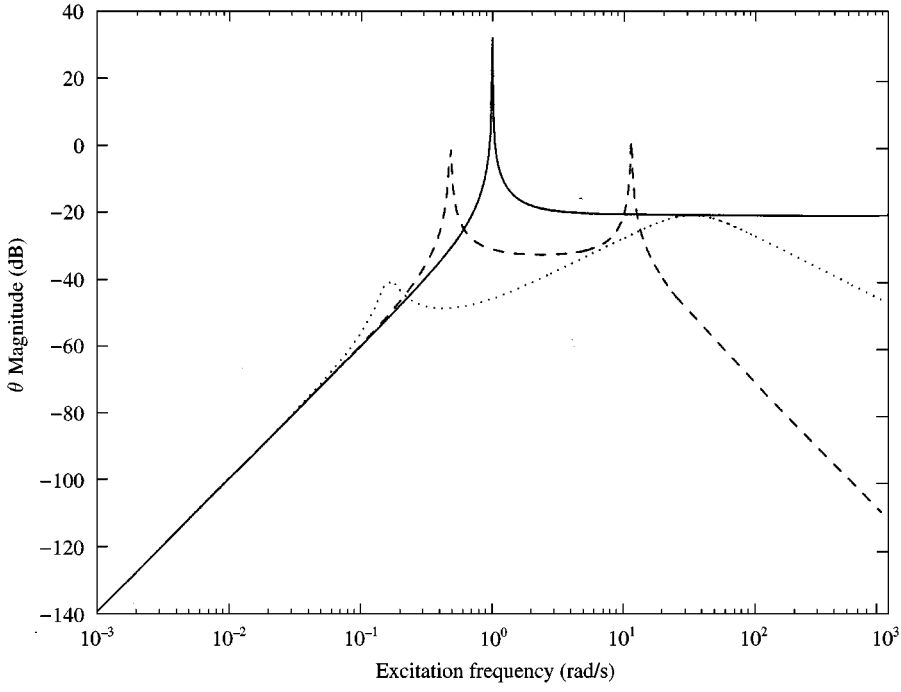

Figure 4. Crane-load responses: —, corresponds to case without filter; – –, corresponds to case with passive filter; · · ·, corresponds to case with active filter.

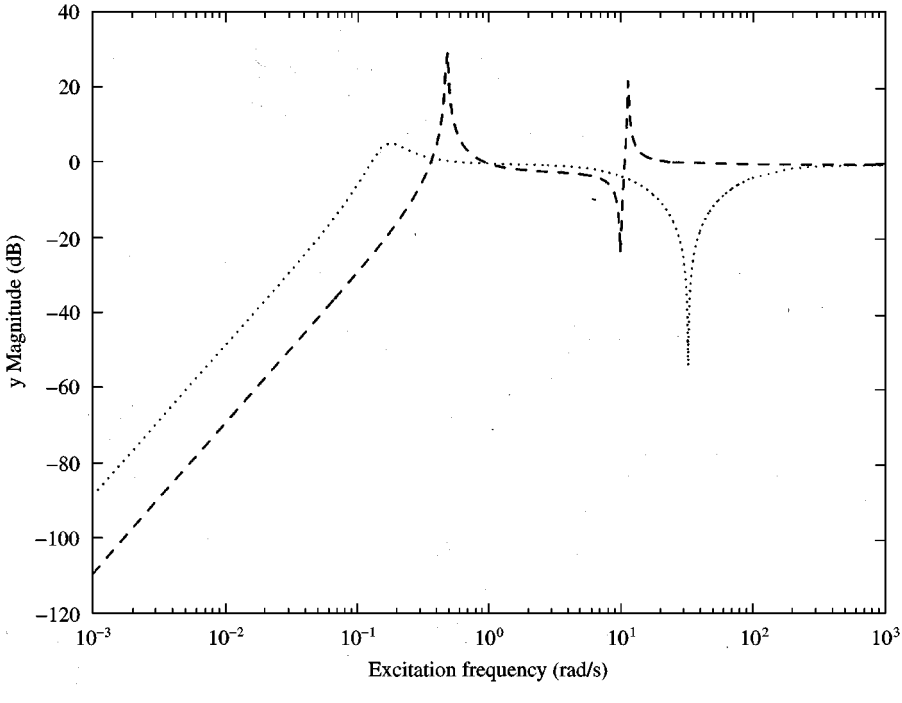

Figure 5. Pivot responses: – –, corresponds to case with passive filter; · · · corresponds to case with active filter.

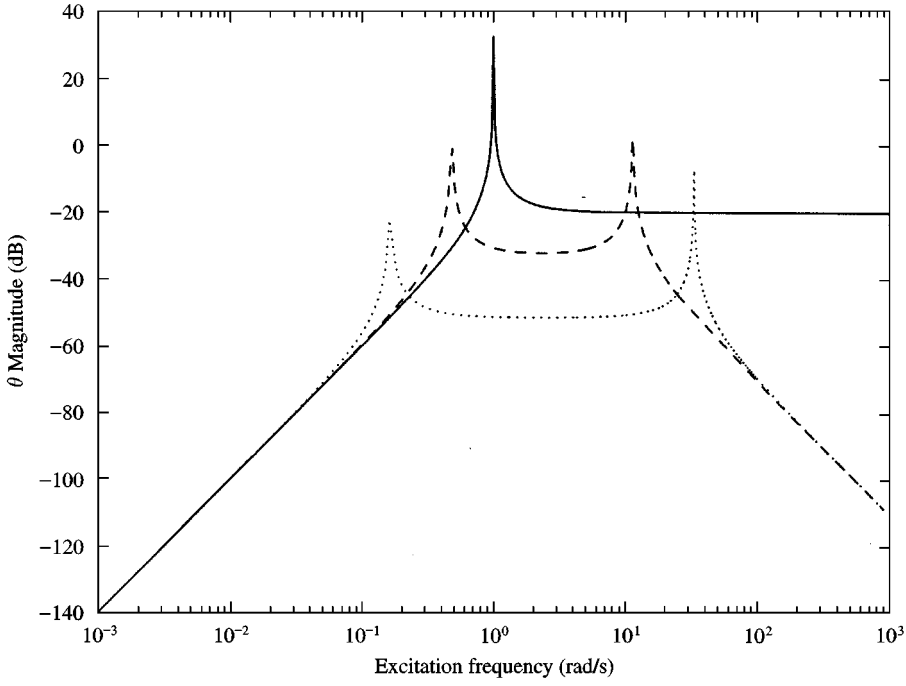

Figure 6. Crane-load responses: —, corresponds to case without filter; – – corresponds to case with passive filter; · · · corresponds to case with active filter.

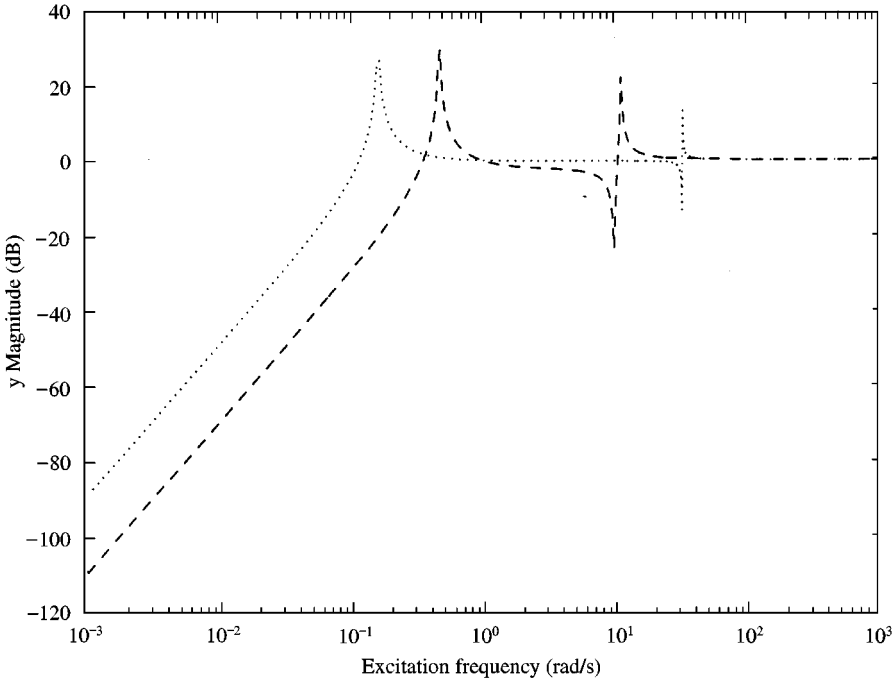

Figure 7. Pivot response: - -, corresponds to case with passive filter; · · ·, corresponds to case with active filter.

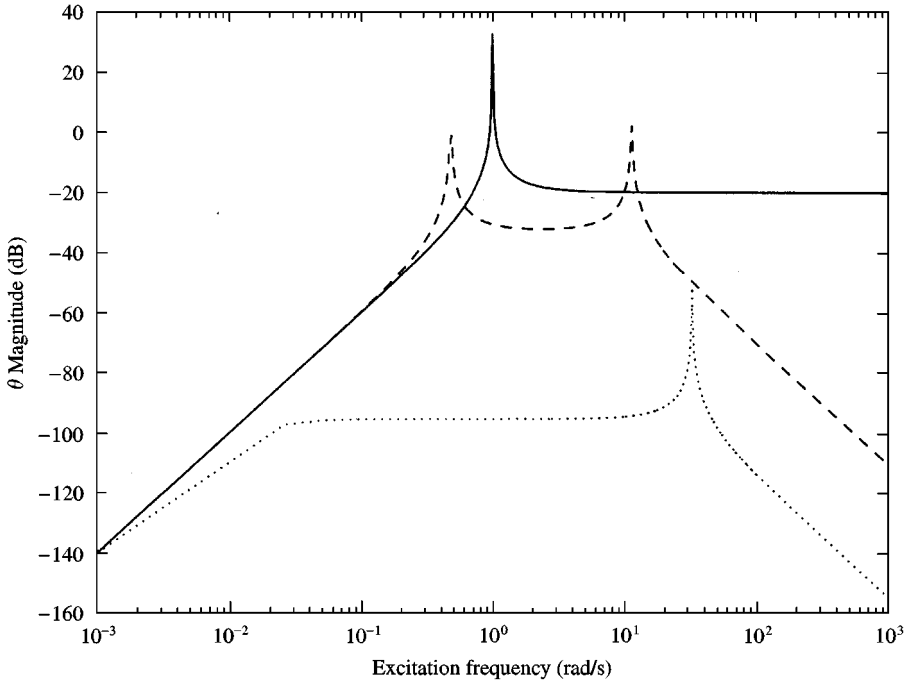

Figure 8. Crane-load responses: —, corresponds to case without filter; - -, corresponds to case with passive filter; · · · corresponds to case with active filter.

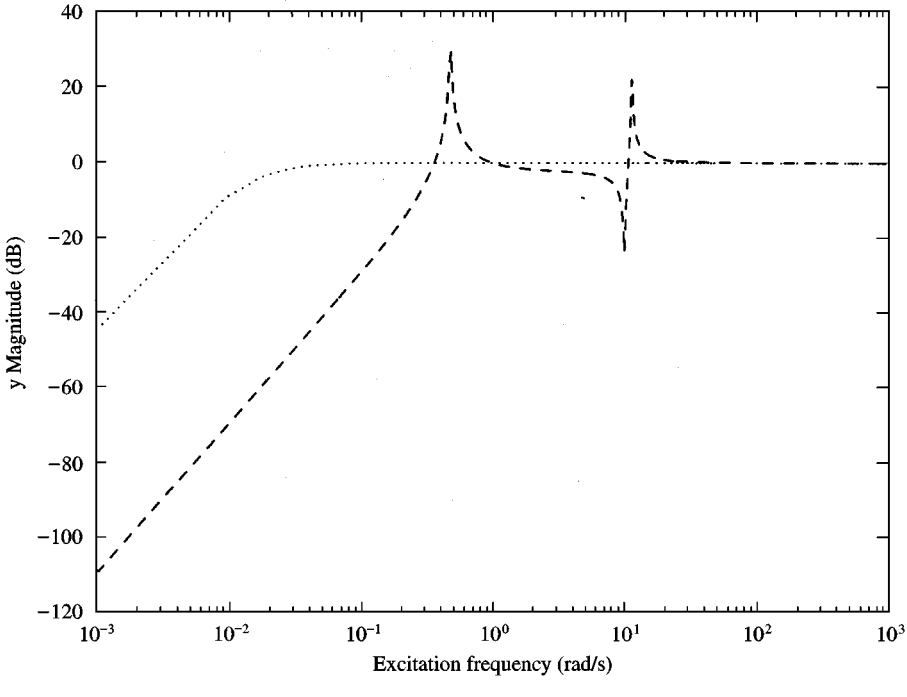

Figure 9. Pivot responses: - -, corresponds to case with passive filter; · · ·, corresponds to case with active filter.

active feedback control, the bandwidth of suppression of the crane-load response is increased significantly. This change in the bandwidth of suppression is related to the changes in the dynamics of the transfer function. These changes are related to the locations of the poles and zeros (see, e.g., reference [25]). In Figure 5, the transfer functions obtained when the horizontal motion of the pivot is treated as an output are shown for the passive and active filter cases. When the filter is passive, the magnitude of horizontal motions of the pivot are quite pronounced, and this situation is not desirable from a practical standpoint if one is to design a reasonably sized track. When the filter is active, the feedback control action is able to substantially attenuate the pivot motions. It is to be noted that in the present case, there is an input component [the second term in equation (10)] that enhances the dissipation in the system.

In Figures 6 and 7, the responses are shown to illustrate the behavior when $B = C = 0$, in equation (10), that is, the control input. Although the crane-load response shown for the active filter case in Figure 6 is highly desirable, the same is not true for the pivot response in the active filter case.

In Figures 8 and 9, the responses are shown for the case when $A = 96{\cdot}2361$, $B = 0$, and $C = 0{\cdot}3$ in equation (10). The proportional feedback component that was zero previously is non-trivial now. Among the three active filter cases treated here, the response characteristics observed in this case are the most desirable because a high attenuation in crane-load response is realized over a large frequency bandwidth. Furthermore, the pivot response characteristics do not show the sharp resonance-like features seen in the previous two cases. If the derivative feedback component in equation (10) is non-trivial, the pivot response shown in Figure 9 can be further attenuated.

Transfer functions were also examined for the parameter values $R_2 = 10$ m, $k/m_1 = 0{\cdot}0$ units, and $m_2/m_1 = 0{\cdot}01$. The corresponding graphs, which are qualitatively similar to those presented in this section, are not included here. Furthermore, detailed inspection of the asymptotes in the low- and high-frequency regions to the different curves and other features of them in Figures 4–9 have been conducted, but they are not included here. The discussion and the results provided in this section by using linearized systems indicate that the mechanical filter can be construed as a vibration absorber to a certain extent. As pointed out in the next section, instabilities do occur in the response of the crane load in certain excitation frequency ranges and certain excitation amplitude ranges. The effect of the mechanical filter on these instabilities is illustrated in the next section.

4. NON-LINEAR ANALYSES

The responses of the systems with and without the filter are illustrated in this section for harmonic and periodic ship-roll motions. The software AUTO94 [24, 26] is used to determine the periodic solutions of the non-linear dynamical systems with and without the filter, and the bifurcations experienced by these solutions with respect to a scalar control parameter are studied. The different control parameters studied include the following: (1) excitation frequency ω, (2)

excitation amplitude F, (3) cable length R_1, and (4) radius of pivot track R_2. For the sake of brevity, the results corresponding to the last two control parameters are not presented here. This section is split into two subsections with the results corresponding to the passive filter case being presented in the first subsection and the results corresponding to the active filter case being presented in the second subsection.

4.1. PASSIVE FILTER

To generate the results shown in Figures 10–12, the excitation frequency was used as a control parameter while the excitation amplitude was held constant at 1·00 m. Sinusoidal excitations are considered in all of the three cases. The amplitude of the periodic response is shown on the y-axis (vertical axis) and the control parameter ω is shown on the x-axis (horizontal axis). Figure 10 corresponds to a case without the filter, and Figures 11 and 12 correspond to cases with the filter. The damping parameter ζ_θ is 0·02 for the case without the filter. Examining the loci of the responses shown in Figure 10, one can observe that cyclic-fold bifurcations occur in an interval close to 1·0 rad/s, which is the linear natural frequency of the planar pendulum in the absence of the filter. The frequency-response curves qualitatively resemble these obtained for a sinusoidally forced Duffing oscillator with a softening spring [24]. In light of the results shown in Figure 10, it is clear that the transfer function shown in Figure 4 for the case without the filter is not representative of the filter behavior over the whole range of the control parameters.

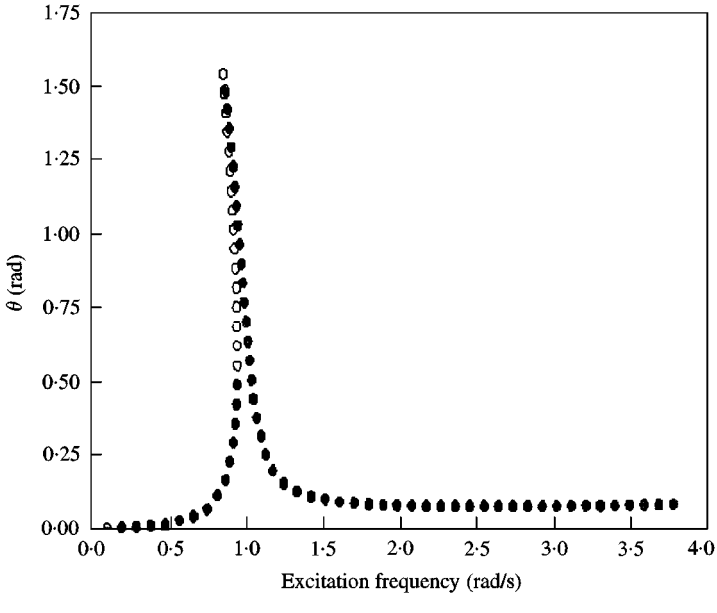

Figure 10. Crane-load responses with the passive filter: ○, unstable periodic motions; ●, stable periodic motions: forcing amplitude $F = 1$ m.

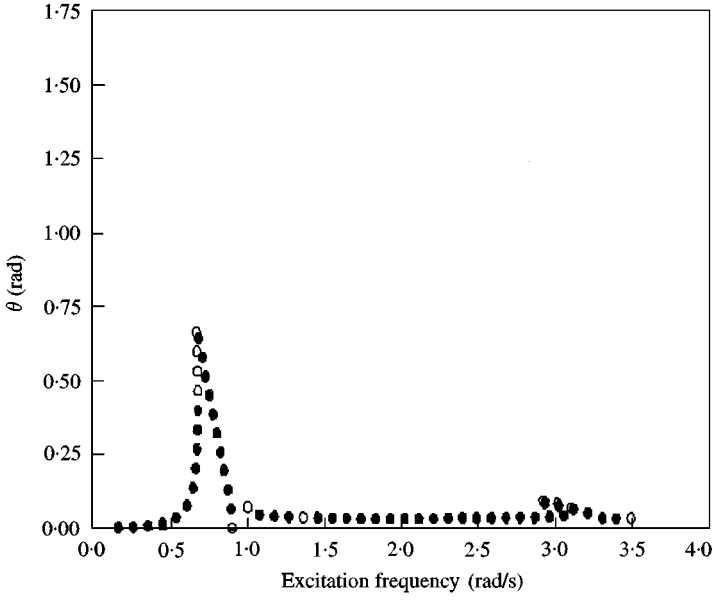

Figure 11. Crane-load responses with the passive filter: ○, unstable periodic motions; ●, stable periodic motions: track radius $R_2 = 10$ m.

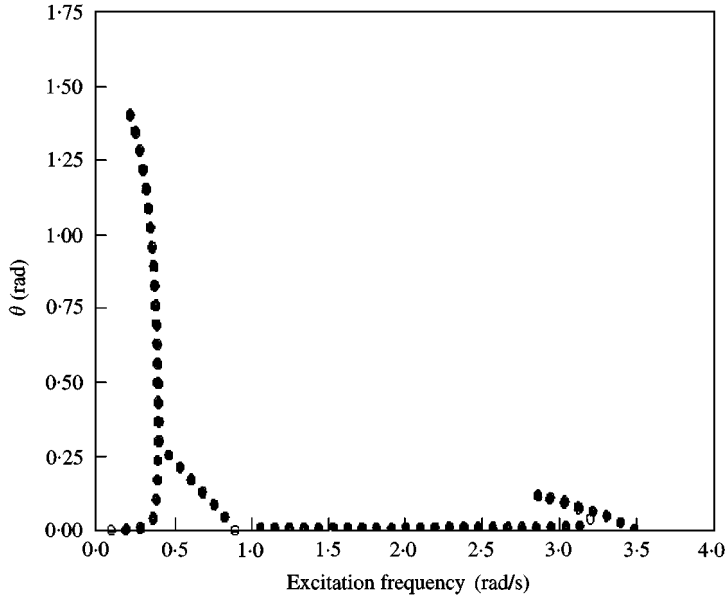

Figure 12. Crane-load responses with the passive filter: ○, unstable periodic motions; ●, stable periodic motions: track radius $R_2 = 50$ m.

The pivot track radius R_2 is respectively 10 and 50 m for the results shown in Figures 11 and 12. In both cases, the mass ratio m_2/m_1 is 0·01, the stiffness parameter k is zero, the damping parameter ζ_θ is 0·02, and the damping parameter ζ_y is zero. Examining the results shown in Figure 11, it is seen that cyclic-fold

bifurcations occur in the response of the crane load in a region to the left of $\omega = 1{\cdot}0$ rad/s. However, comparing the bifurcation points in this case with those shown in Figure 10, it is clear that the bifurcation locations are shifted by the presence of the filter. (The unshaded circles seen in the range of $\omega = 1{-}1{\cdot}5$ in Figure 11 actually correspond to stable solutions, whose presence were ascertained through numerical integrations. The aberrations seen here are to do with the step size selection and/or the initial point used with the continuation software). The presence of the filter introduces some bifurcations close to $\omega = 3{\cdot}0$ rad/s, which on examining equations (6) and (7) may be possible due to non-linear resonances. (These bifurcation points are quite prominent when the loci of the responses is examined in a window around $\omega = 3{\cdot}0$ rad/s.) The magnitude of the crane-load response is substantially attenuated in the presence of the filter.

When the filter track radius is increased to 50 m, the crane-load response in the vicinity of $\omega = 1{\cdot}0$ rad/s is substantially reduced. The bifurcation points seen to the left of $\omega = 1{\cdot}0$ rad/s in Figure 10 are shifted further to the left and the presence of the cyclic-fold bifurcation points are not clearly discernible in Figure 12. There are two cyclic-fold bifurcation points that occur in the range of $\omega = 3{\cdot}0{-}3{\cdot}5$ rad/s. The results shown in Figure 12 indicate that the transfer functions presented in Figure 4 for the system with the passive filter is not representative of the system behaviour over the whole range of control parameters.

In Figures 13–18, the responses of the dynamical systems with and without the filter are shown when the excitation amplitude is used as a control parameter while keeping the excitation frequency fixed. For all of the results corresponding to Figures 13, 14, and 16–18, sinusoidal excitations [i.e., equation (8)] are used. The results shown in Figure 15 correspond to periodic excitations of the form of

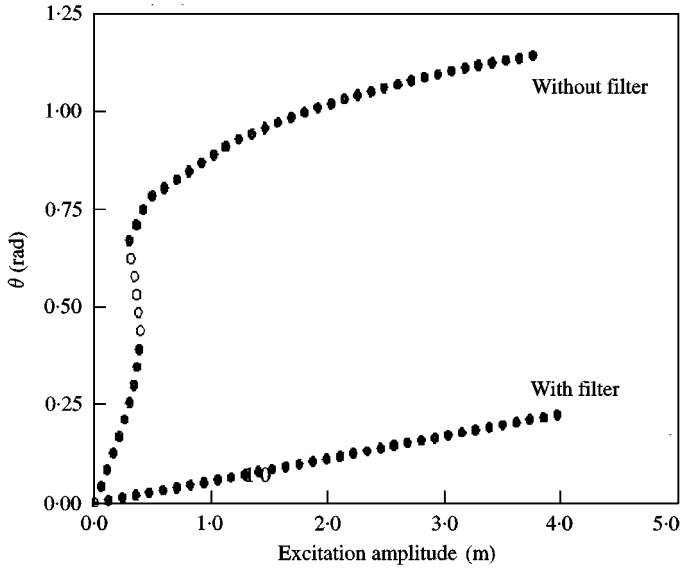

Figure 13. Crane-load responses with the passive filter ($R_2 = 10$, $m_2/m_1 = 0{\cdot}01$): ○, unstable periodic motions; ●, stable periodic motions: excitation frequency $\omega = 0{\cdot}97$ rad/s.

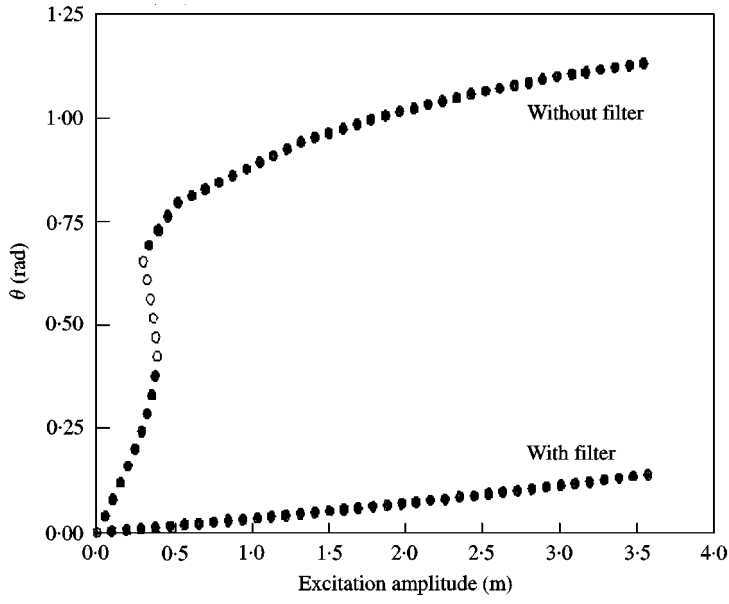

Figure 14. Crane-load responses with the passive filter ($R_2 = 50$ m, $m_2/m_1 = 0{\cdot}01$, $K/m_1 = 0{\cdot}4$): ○, unstable periodic motions; ●, stable periodic motions: excitation frequency $\omega = 0{\cdot}97$ rad/s.

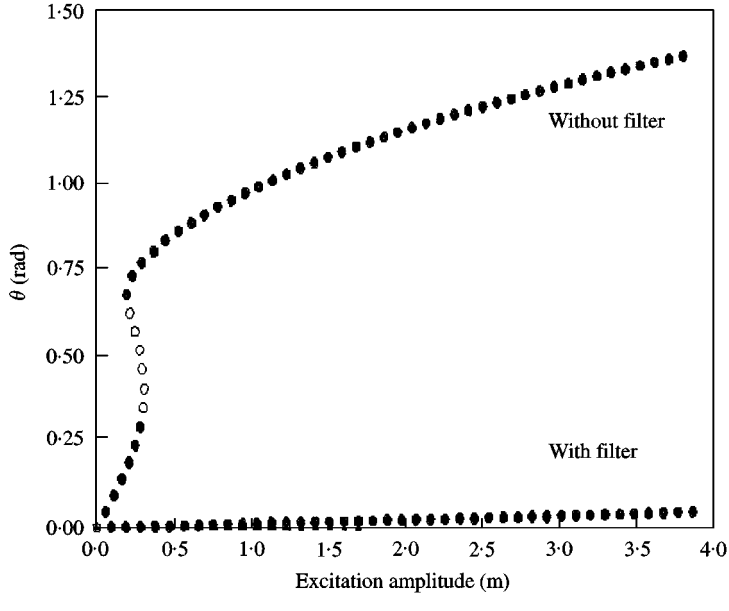

Figure 15. Crane-load responses with the passive filter ($R_2 = 50$ m, $m_2/m_1 = 0{\cdot}01$): ○, unstable periodic motions; ●, stable periodic motions: periodic excitation with components at 0·97, 1·94, and 2·91 rad/s.

equation (9). The excitation frequency corresponding to Figure 13 is 0·97 rad/s. For the results corresponding to the system with the filter, the track radius is 10 m, the stiffness parameter $k = 0{\cdot}0$, and the mass ratio m_2/m_1 is 0·01. The cyclic-fold bifurcations that occur in the response of the crane load when the filter is absent are

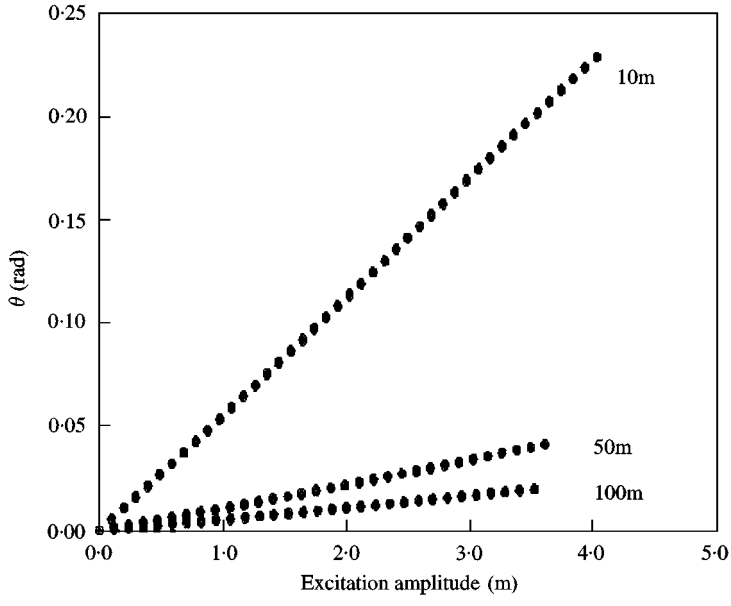

Figure 16. Crane-load responses with and without the passive filter: ○, unstable periodic motions; ●, stable periodic motions: excitation frequency $\omega = 0{\cdot}97$ rad/s.

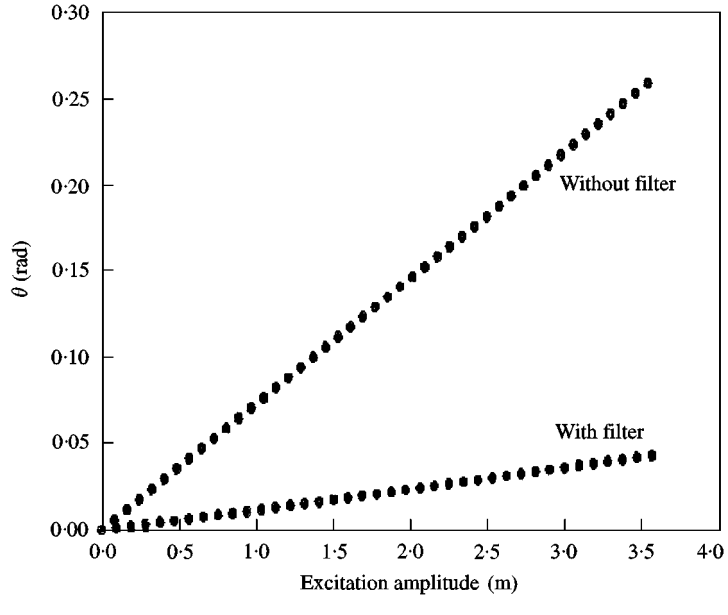

Figure 17. Crane-load responses with ($R_2 = 50$ m, $m_2/m_1 = 0{\cdot}01$) and without the passive filter: ○, unstable periodic motions; ●, stable periodic motions: excitation frequency $\omega = 0{\cdot}77$ rad/s.

eliminated through introduction of the filter. For $R_2 = 10$ m and $k = 0{\cdot}0$ N/m, when the transfer functions for the linear systems corresponding to the cases without the filter and with the passive filter are examined, the respective gains at $\omega = 0{\cdot}97$ rad/s turn out to be about 5 dB and -19 dB. For the system without the

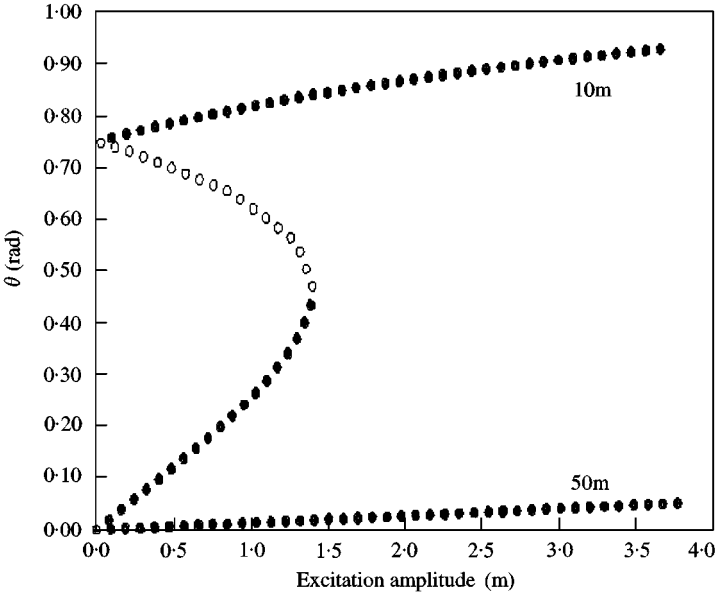

Figure 18. Crane-load responses with the passive filter: ○, unstable periodic motions; ●, stable periodic motions: excitation frequency $\omega = 0{\cdot}67$ rad/s.

filter, returning to Figure 13, it is seen that prior to the first cyclic-fold bifurcation point, that is, for excitation amplitudes less than 0·4 m, the magnitude of the crane-load response is in agreement with the magnitude computed by using the 5 dB gain. Hence, the system without the filter can be represented by a linear dynamical system for $F < 0{\cdot}4$ m. For the system with the passive filter, the results shown in Figure 13 are in agreement with the magnitudes computed by using the −19 dB gain. Hence, at the excitation frequency of 0·97 rad/s, the system with the passive filter effectively behaves like a linear system.

The results shown in Figure 14 are qualitatively similar to those presented in Figure 13 except that the filter parameters are different in this case. Here, the filter parameters are as follows: (1) $R_2 = 50$ m, (2) $k/m_1 = 0{\cdot}4$ units, and (3) $m_2/m_1 = 0{\cdot}01$. Again, there are cyclic-fold bifurcations in the response of the crane load in the absence of the filter. These bifurcations, which are subcritical, are eliminated through introduction of the passive filter. With the passive filter, the system behaves in a linear manner.

The bifurcation diagrams for the systems with and without the passive filter for a case of periodic excitation with a fundamental frequency of 0·97 rad/s are illustrated in Figure 15. The form of the excitation is given by equation (9). Second and third harmonics of the fundamental frequency were chosen because of the form of the non-linearities in equations (1), (6), and (7). Subcritical bifurcations do occur in the response of the crane load in the absence of the filter. In the presence of a filter with a pivot track radius of 50 m, mass ratio of $m_2/m_1 = 0{\cdot}01$, and stiffness parameter $k = 0$, the subcritical bifurcations are eliminated in the response and the system behaves in a linear manner in the considered window of parameters.

In Figure 16, the responses of the crane load when the system has a passive filter are plotted for the following values of the pivot track radius: (1) $R_2 = 10$ m, (2) $R_2 = 50$ m, and (3) $R_2 = 100$ m. The system with the passive filter effectively behaves like a linear system for different values of R_2 at the excitation frequency of 0·97 rad/s.

In Figure 17, the variation of amplitudes of the periodic responses with respect to the excitation amplitude are shown for systems without a filter and with a passive filter. The excitation frequency is held fixed at is held fixed as 0·77 rad/s, and for the system with the filter, $R_2 = 50$ m, $k = 0$ N/m, and $m_2/m_1 = 0{\cdot}01$. From linear analyses, it is known that the transfer function gains are -16 dB and -32 dB for the systems without the filter and with the passive filter respectively. The magnitudes predicted by using these transfer function gains are in agreement with the results shown in Figure 15 indicating that the systems with and without the filter behave linearly for the considered parameter values.

In Figure 18, the effect of varying the pivot track radius is illustrated when the excitation frequency is 0·67 rad/s. The subcritical bifurcations that occur at

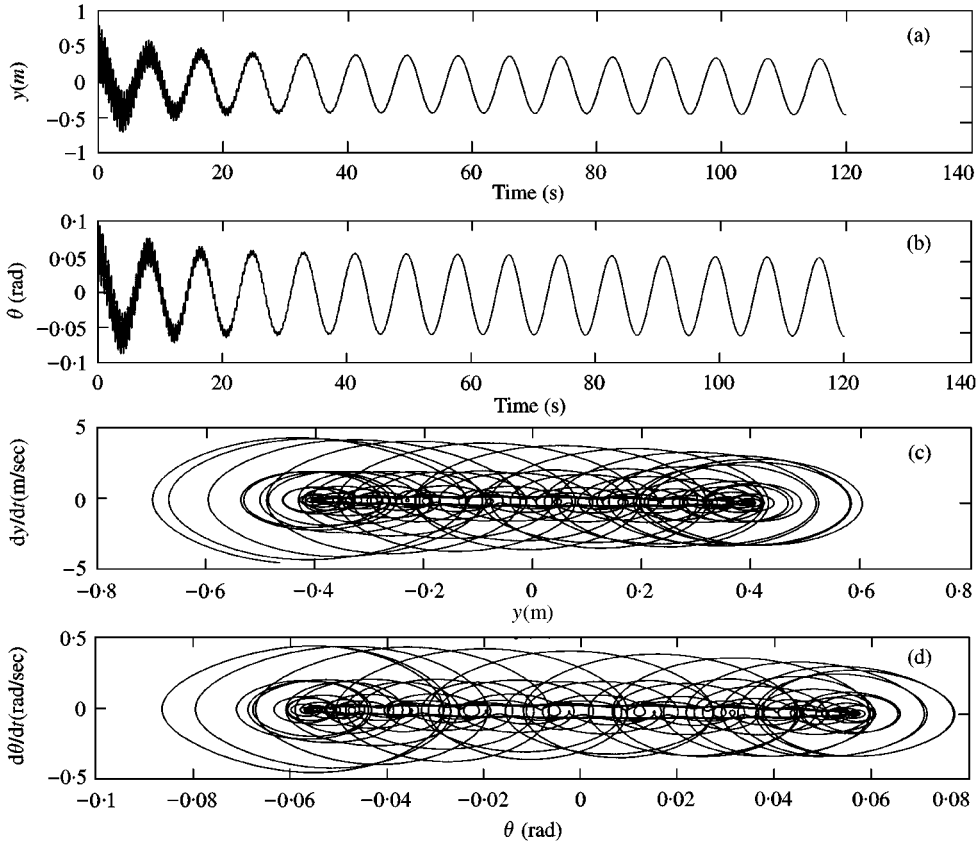

Figure 19. Responses with the passive filter: (a) time history of pivot motion, (b) time history of crane-load motion, (c) motion in y–$\dot{y}$ plane, and (d) motion in θ–$\dot{\theta}$ plane. Initial condition $(y, \dot{y}, \theta, \dot{\theta}) = (0{\cdot}0, 0{\cdot}0, 0{\cdot}1, 0{\cdot}0)$.

$R_2 = 10$ m are eliminated when the pivot track radius is 50 m. From linear analyses, it is known that the transfer function gain at 0·67 rad/s is -6 dB for $R_2 = 10$ m and -32 dB for $R_2 = 50$ m. The magnitudes predicted by using the gain of -32 dB at $R_2 = 50$ m are in agreement with the results shown in Figure 18. Thus, the system with the passive filter behaves in a linear manner throughout the considered range of excitation amplitudes at $R_2 = 50$ m but not so at the lower value of $R_2 = 10$ m.

Other numerical studies were also considered to examine the behavior of the systems with and without the filter at other excitation frequencies. At an excitation frequency of 2·0 rad/s, in the system without the filter, the crane load response experiences a pitchfork bifurcation at about $F = 0{\cdot}12$ m when the excitation amplitude is used as a control parameter. The response curves indicate that a principal parametric resonance [24] is active at this excitation frequency. After the introduction of a passive filter with a pivot track radius of 10 m and a stiffness $k = 0{\cdot}0$ N/m, the response grows monotonically and no bifurcations occur as the excitation amplitude is increased. The behavior typical of a parametric resonance is no longer present. When the stiffness parameter k is increased from zero, bifurcations do occur in the response of the crane load in the presence of the filter. For $k/m_1 = 0{\cdot}4$ units, these bifurcations are cyclic-fold bifurcations.

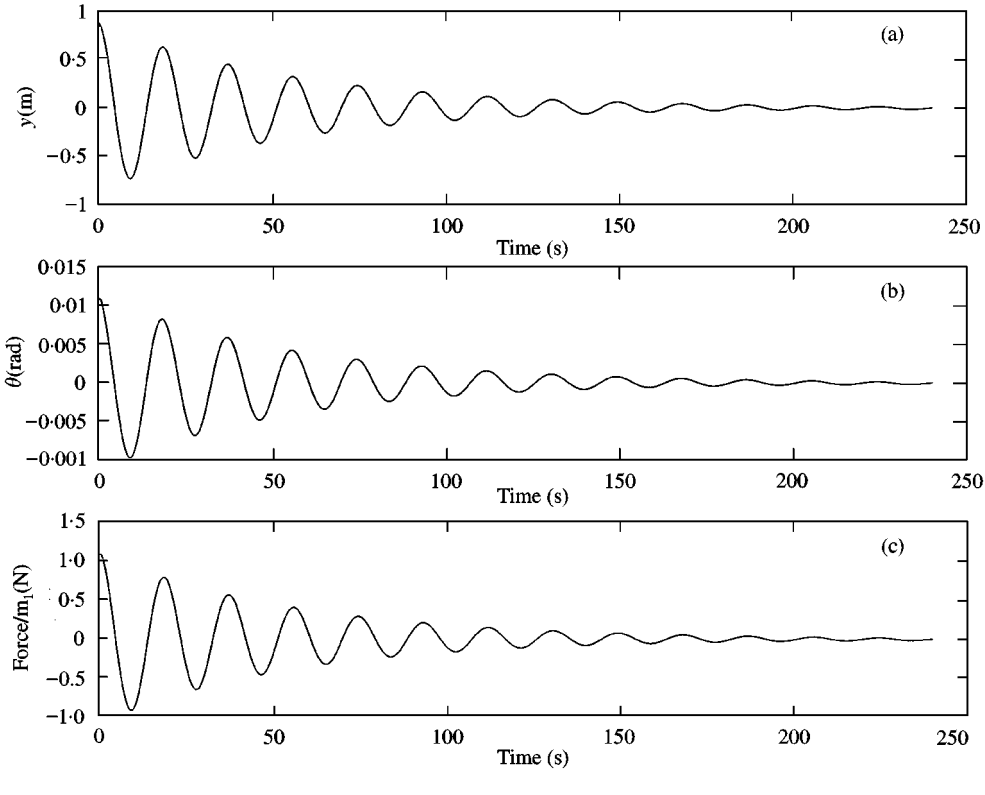

Figure 20. Responses with the active filter: (a) pivot motion, (b) crane load motion, and (c) control force. Initial conditions $(y, \dot{y}, \theta, \dot{\theta}) = (0{\cdot}0, 0{\cdot}0, 0{\cdot}1, 0{\cdot}0)$.

In this section, the characteristics of dynamics of the system with a passive filter has been compared with the characteristics of dynamics of the corresponding system without a filter. Thus far, in this section as well as in section 2, the steady state behavior of the considered system was examined in detail. In the next section, control of transient oscillations of the crane load is considered and it is shown that the presence of an active filter is advantageous for controlling such oscillations.

4.2. ACTIVE FILTER

Here, the active filter case with the feedback control law (10) is considered with $A = 96{\cdot}2361$, $B = -0{\cdot}5$, and $C = 0$. Time histories and phase portraits are shown in Figure 19 for a passive filter with a track radius of 10 m, $m_2/m_1 = 0{\cdot}01$, and a stiffness parameter $k/m_1 = 0{\cdot}4$ units. In this case, large excursions in the pivot motions and the crane load motions are clearly discernible when the initial

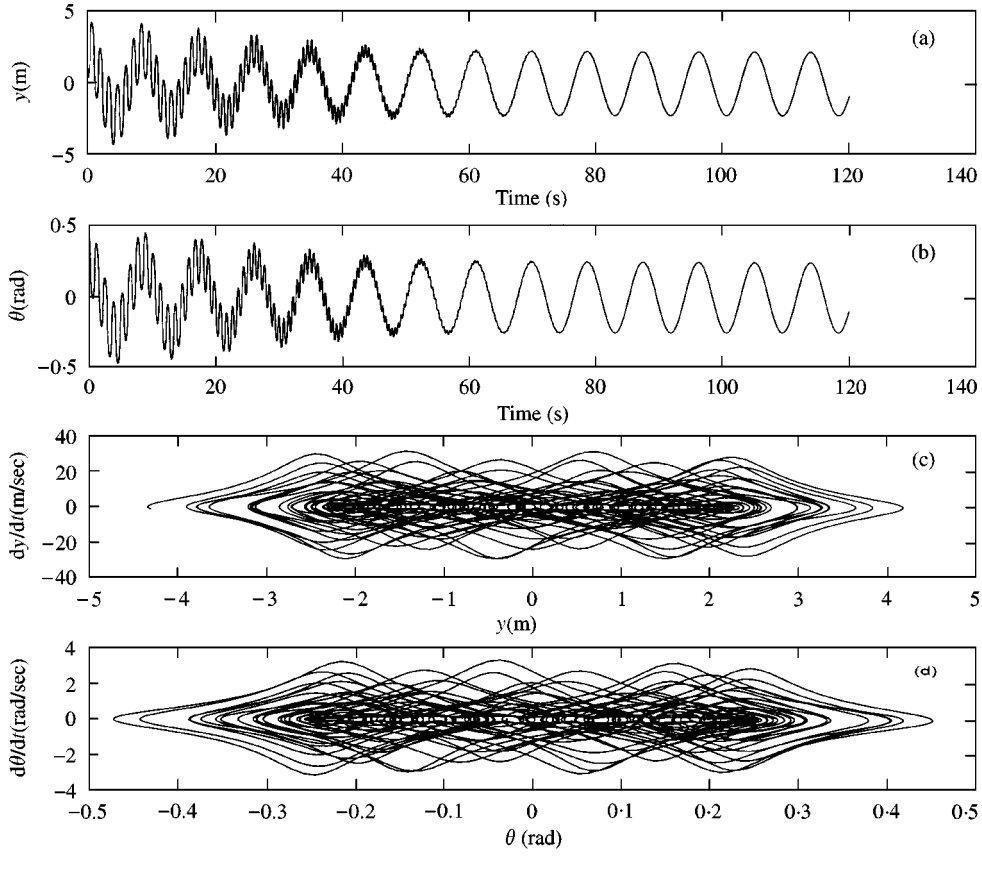

Figure 21. Responses with the passive filter: (a) time history of pivot motion, (b) time history of crane-load motion, (c) motion in y–$\dot{y}$ plane, and (d) motion in θ–$\dot{\theta}$ plane. Initial condition $(y, \dot{y}, \theta, \dot{\theta}) = (0{\cdot}0, 0{\cdot}0, 0{\cdot}5, 0{\cdot}0)$.

condition is non-trivial. This type of initial condition can occur when there is an offset in the crane-load position due to a wind gust or another disturbance.

It is to be noted that the dissipation in the passive filter system is low. In Figure 20, the time histories of the pivot motions, the crane load motions, and the force input to the pivot/crane load mass are shown for the active filter case. The oscillations are attenuated rapidly. Clearly, if the magnitude of B was larger in the control law (10), the pivot motions as well as the load motions will be reduced in magnitude more rapidly. The high-frequency oscillations seen in the initial phase of the motions when the filter is passive are absent in the active filter case. This is to do with the dissipation introduced by the feedback control.

The results of Figures 21 and 22, which are similar to results of Figures 19 and 20, were obtained when the filter track radius was kept the same while the stiffness parameter k/m_1 was decreased to 0·1 units. The elastic restraints on the pivot are softer compared to the earlier case. The initial condition was also changed from the previous case.

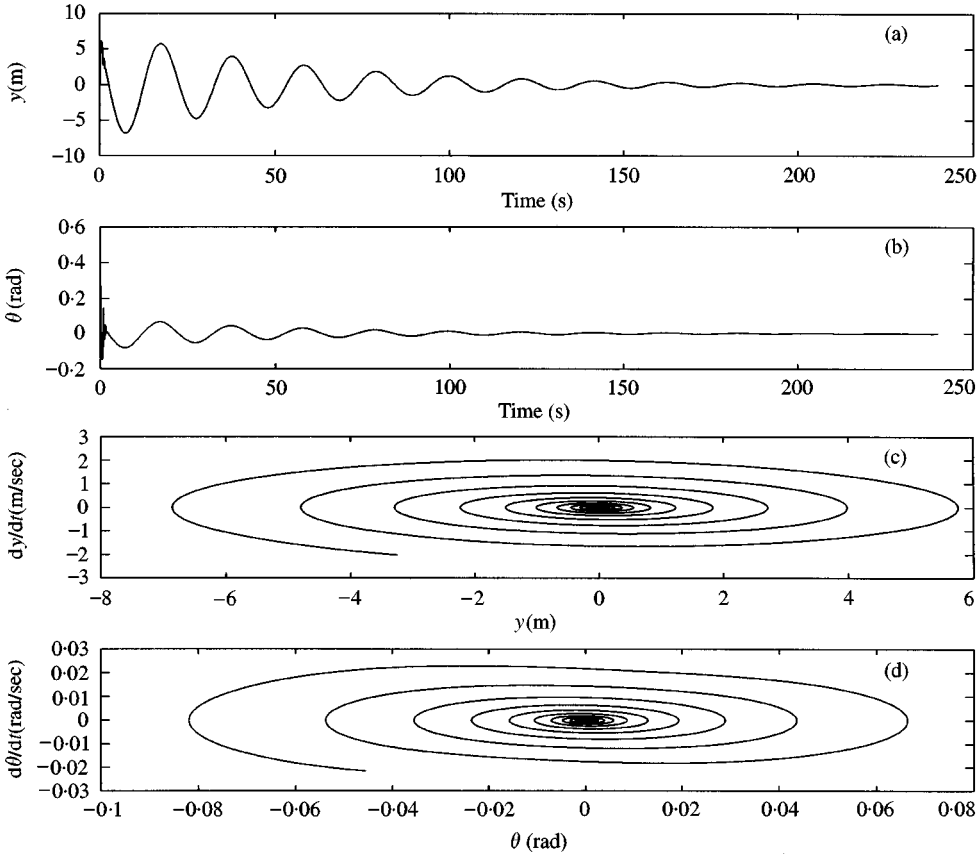

Figure 22. Responses with the active filter: (a) time history of pivot motion, (b) time history of crane-load motion, (c) motion in y–$\dot{y}$ plane, and (d) motion in θ–$\dot{\theta}$ plane. Initial condition $(y, \dot{y}, \theta, \dot{\theta}) = (0{\cdot}0, 0{\cdot}0, 0{\cdot}5, 0{\cdot}0)$.

Again, high-frequency oscillations are discernible in the initial phase of the motions in the passive filter case. The responses in the active filter case are illustrated in Figure 22. It is clear from the time histories and the phase portraits that the pivot and crane load motions are rapidly attenuated when the filter is active.

The results of Figures 23–26 are illustrative of the effectiveness of the active filter when the initial condition is non-trivial and when periodic forcing is also present. The filter is characterized by a track radius of 10 m, a mass ratio $m_2/m_1 = 0{\cdot}01$, and a stiffness parameter $k/m_1 = 0{\cdot}1$ units for the results corresponding to Figures 23 and 24. Furthermore, in these cases, the excitation is sinusoidal with a frequency of 0·97 rad/s and amplitude of 1·0 m. Clearly, on comparing the results shown in Figures 23 and 24, the effectiveness of the active filter in attenuating the pivot and the crane-load motions is discernible.

The results shown in Figures 25 and 26 correspond to a case with non-trivial initial condition and a periodic excitation of the form (9). The fundamental

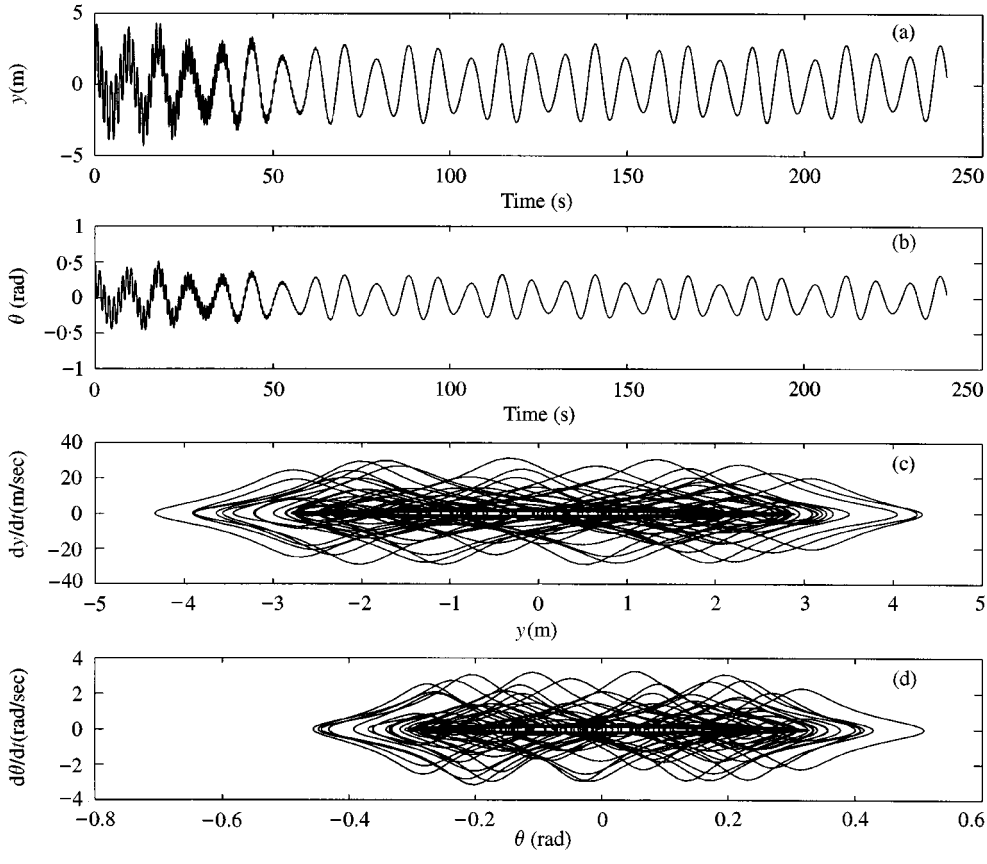

Figure 23. Forced oscillations with the passive filter: (a) time history of pivot motion, (b) time history of crane-load motion, (c) motion in y–$\dot{y}$ plane, and (d) motion in θ–$\dot{\theta}$ plane. Initial condition $(y, \dot{y}, \theta, \dot{\theta}) = (0{\cdot}0, 0{\cdot}0, 0{\cdot}5, 0{\cdot}0)$, excitation frequency $\omega = 0{\cdot}97$ rad/s, and excitation amplitude $F = 1{\cdot}0$ m.

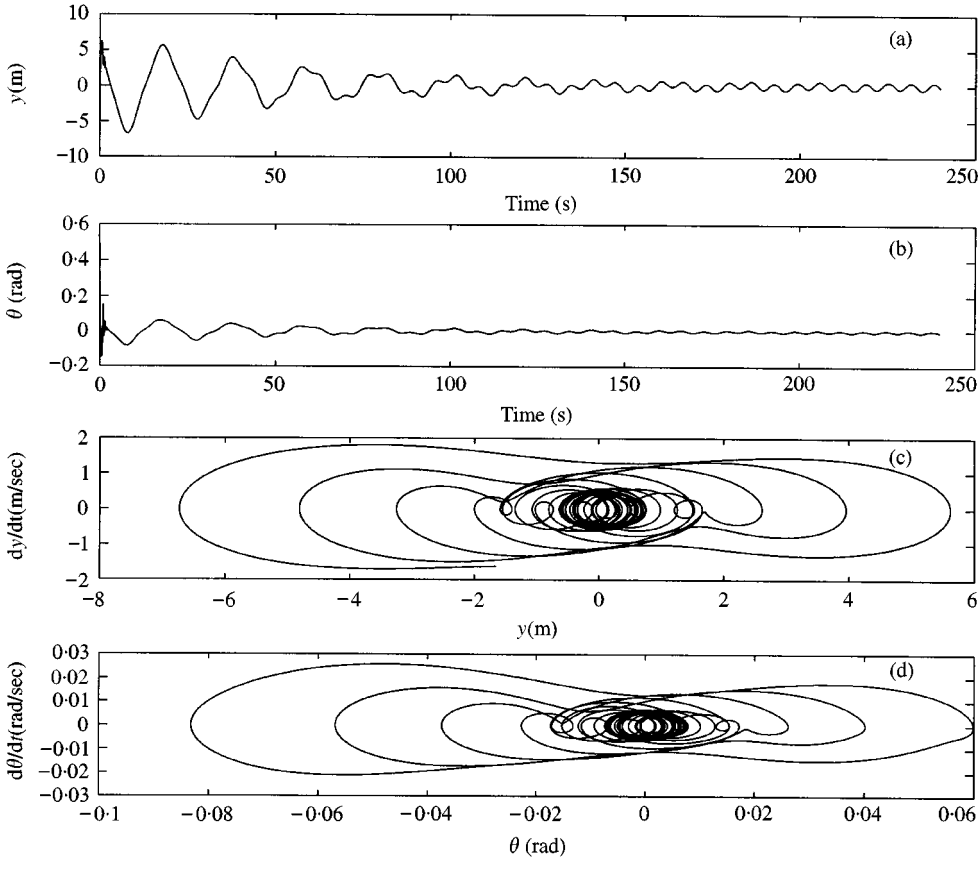

Figure 24. Forced oscillations with the active filter: (a) time history of pivot motion, (b) time history of crane-load motion, (c) motion in y–$\dot{y}$ plane, and (d) motion in θ–$\dot{\theta}$ plane. Initial condition $(y, \dot{y}, \theta, \dot{\theta}) = (0{\cdot}0, 0{\cdot}0, 0{\cdot}5, 0{\cdot}0)$, excitation frequency $\omega = 0{\cdot}97$ rad/s, and excitation amplitude $F = 1{\cdot}0$ m.

frequency is 0·97 rad/s. Furthermore, the elastic restraint parameter k/m_1 is now assigned a value of 0·1 units. The other filter parameters are the same as in the earlier case.

The effectiveness of the active filter is again clearly discernible when the time histories and phase portraits in Figure 26 are compared with the corresponding plots in Figure 25. Simulations were also conducted for other excitation frequencies and excitation amplitudes and other non-trivial initial conditions. The results obtained in these cases and the bifurcation diagrams shown in Figures 27 and 28 are illustrative of the effectiveness of the performance of the active filter.

5. CONCLUDING REMARKS

The concept of a mechanical filter has been introduced in this study, and the application of this concept for controlling ship–crane-load oscillations has been

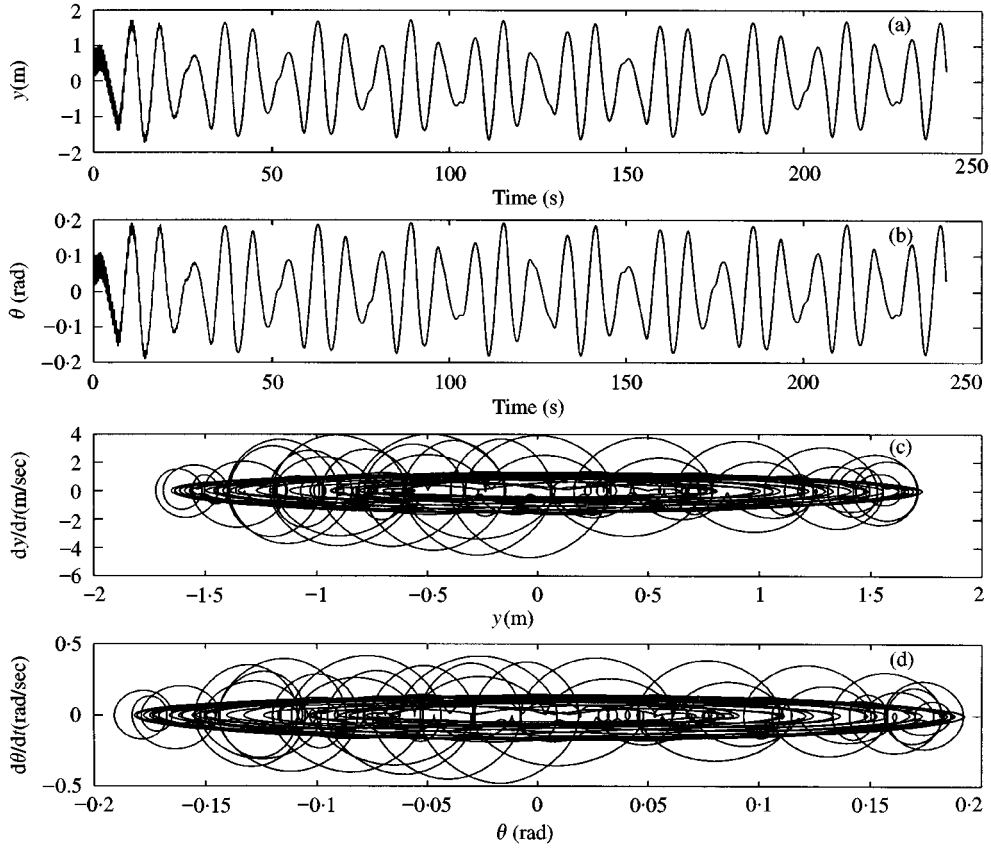

Figure 25. Forced oscillations with the passive filter: (a) time history of pivot motion, (b) time history of crane-load motion, (c) motion in y–$\dot{y}$ plane, and (d) motion in θ–$\dot{\theta}$ plane. Initial condition $(y, \dot{y}, \theta, \dot{\theta}) = (0{\cdot}0, 0{\cdot}0, 0{\cdot}5, 0{\cdot}0)$, $F = 1{\cdot}0$ m, and excitation with components at 0·97, 1·94, and 2·91 rad/s.

considered with the aid of numerical simulations. The filter has been introduced at the pivot point about which the load oscillations occur on the premise that by controlling the motions of the pivot, one can effectively control the crane-load motions. Here, through introduction of the mechanical filter, the pivot is constrained to follow a certain geometric path in space. Both linear and non-linear dynamical systems corresponding to the systems with and without the filter have been examined. The linear dynamical systems are useful for illustrating the similarities between mechanical filters and vibration absorbers and mechanical filters and electrical filters. Analyses of the non-linear dynamical systems show that the proposed mechanical filter concept for a ship crane vessel is promising for suppressing subcritical bifurcations and shifting bifurcation points in the response of the crane load to periodic ship-roll motions. A static feedback control law was considered in the realization of an active filter and it is illustrated that the active filter is helpful for attenuating transient crane load oscillations besides steady state oscillations. In work in progress, perturbation analysis is being used to obtain

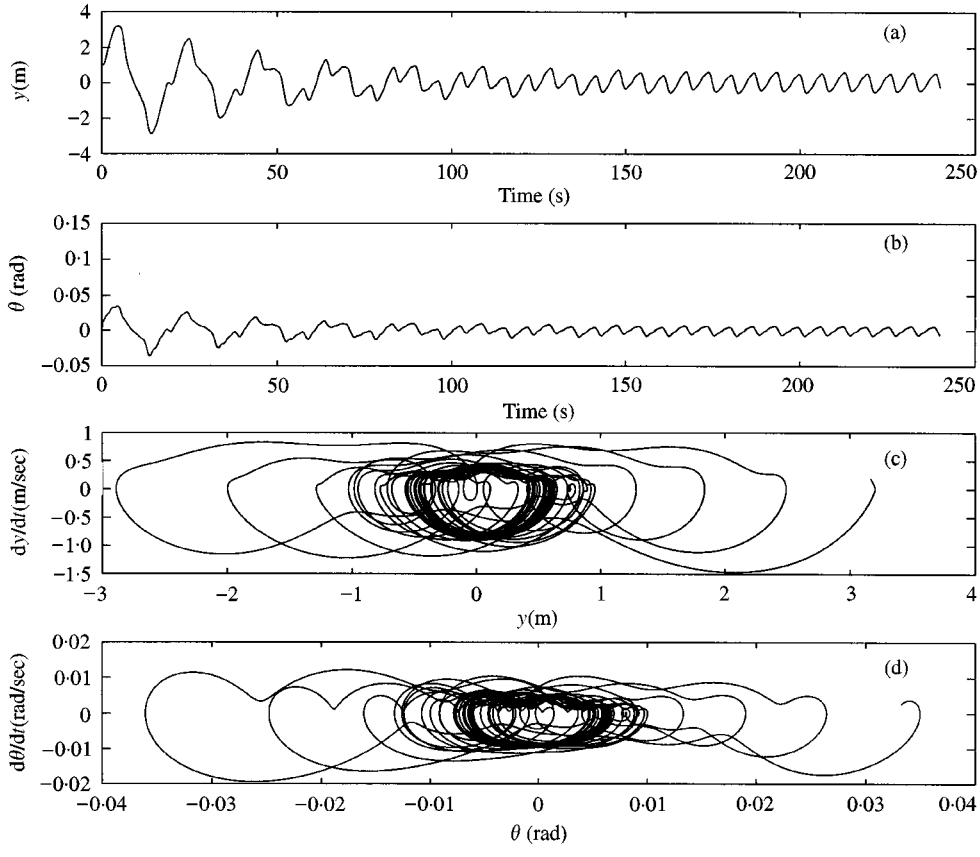

Figure 26. Forced oscillations with the active filter: (a) time history of pivot motion, (b) time history of crane-load motion, (c) motion in y–$\dot{y}$ plane, and (d) motion in θ–$\dot{\theta}$ plane. Initial condition $(y, \dot{y}, \theta, \dot{\theta}) = (0{\cdot}0, 0{\cdot}0, 0{\cdot}5, 0{\cdot}0)$, $F = 1{\cdot}0$ m, and excitation with components at 0·97, 1·94, and 2·91 rad/s.

approximate solutions for "small" θ and "small" y motions about the trivial equilibrium position. These approximate solutions can be used to understand the system responses in the presence of an external resonance. In the current work, no formal and systematic procedure has been presented for the design of a mechanical filter for a ship crane vessel. It is hoped that this issue can be addressed in future work. Furthermore, a realistic analysis should allow for crane-load oscillations in a three-dimensional space and other considerations such as the crane load cable elasticity, boom stiffness, etc. These issues are currently being explored. It is believed that the proposed mechanical filter concept has wide applicability.

ACKNOWLEDGMENTS

Support received for this work from the U.S. Office of Naval Research through contract No. N00014-96-1-1123 is gratefully acknowledged. Dr Kam Ng is the technical monitor for this contract.

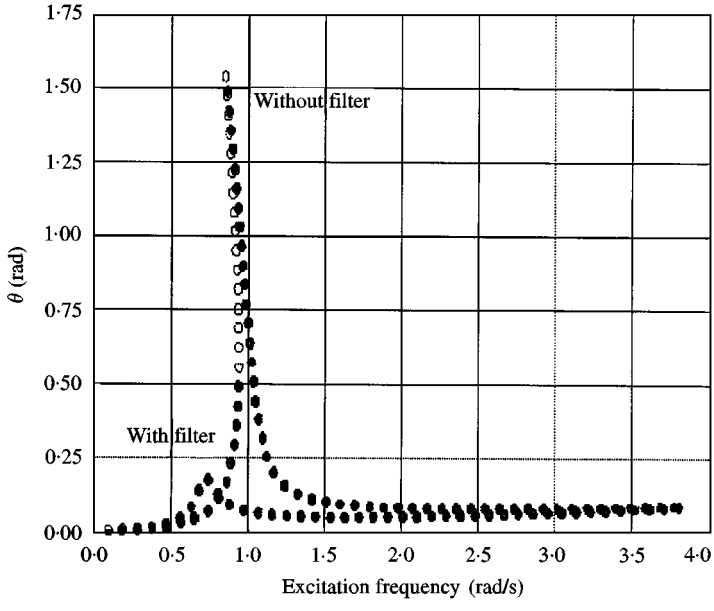

Figure 27. Crane-load responses with ($R_2 = 10$ m) and without the active filter: ○, unstable periodic motions; ●, stable periodic motions: track radius $R_2 = 10$ m.

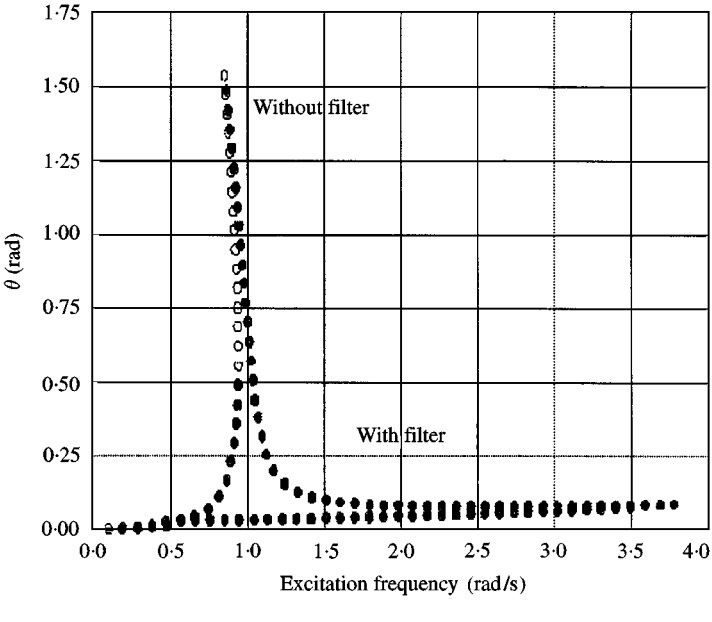

Figure 28. Crane-load responses with ($R_2 = 50$ m) and without the active filter: ○, unstable periodic motions; ●, stable periodic motions: track radius $R_2 = 50$ m.

REFERENCES

1. M. H. Patel, D. T. Brown and J. A. Witz 1987 *Transactions of the Royal Institution of Naval Architects* **129**, 103–113. Operability analysis for a monohull crane vessel.

2. F. J. McCormick and J. A. Witz 1993 *Underwater Technology* **19**, 30–39. An investigation into the parameter excitation of suspended loads during crane vessel operations.
3. J. A. Witz 1995 *Ocean Engineering* **22**, 411–420. Parametric excitation of crane loads in moderate sea states.
4. C. Chin and A. H. Nayfeh 1996 *Proceedings of the 37th AIAA/ASME/ASCE/AHS/ASC Structures, Structural Dynamics, and Materials Conference, AIAA Paper No.* 96-1485. *Salt Lake City, Utah*, 15–17 *April*. Nonlinear dynamics of crane operation at sea.
5. J. W. Auernig and H. Troger 1987 *Automatica* **23**, 437–447. Time optimal control of overhead cranes with hoisting of the load.
6. K. A. F. Moustafa and A. M. Ebeid 1988 *Transactions of the ASME Journal of Dynamic Systems, Measurement, and Control* **110**, 266–271. Nonlinear modeling and control of overhead crane load sway.
7. B. D'Andréa-Novel and J. Levine 1990 *Proceedings of the International Symposium MTNS-89,* Vol. II, 523–529. Modelling and nonlinear control of an overhead crane.
8. A. M. Ebeid, K. A. F. Moustafa and H. E. Emara-Shabaik 1992 *International Journal of Systems Science* **23**, 2155–2169. Electromechanical modelling of overhead cranes.
9. M. Fleiss, J. Levine and P. Rouchon 1991 *IEEE Proceedings of the 30th Conference on Decision and Control, Brighton, England*, 736–741. A simplified approach of crane control via a generalized state-space model.
10. Y. Sakawa and A. Nakazumi 1985 *Transactions of the ASME Journal of Dynamic Systems, Measurement, and Control* **107**, 200–206. Modeling and control of a rotary crane.
11. R. Souissi and A. J. Koivo 1992 *First IEEE Conference on Control Applications, Dayton, OH*, 782–787. Modeling and control of a rotary crane for swing-free transport of payloads.
12. G. G. Parker, B. Petterson, C. R. Dohrmann and R. D. Robinett 1995 *Proceedings of the Smart Structures and Materials Symposium on Industrial and Commercial Applications of Smart Structures Technologies*, vol. 2447, *San Diego, CA*, 131–140. Vibration suppression of fixed-time jib crane maneuvers.
13. McGraw-Hill 1997 *Encyclopedia of Science and Technology* New York: McGraw-Hill.
14. I. Iwasaki, K. Tanida, S. Kaji and M. Mutaguchi 1997 *Proceedings of the DETC'97 ASME Design Engineering Technical Conferences* DETC97/VIB-3816, Sacremento, CA., 1–8. Development of an active mass damper for stabilizing the load suspended on a floating crane.
15. J. P. Hartog 1985 *Mechanical Vibrations* New York: Dover
16. F. R. Arnold 1955 *Journal of Applied Mechanics* **20**, 487–492. Steady-state behavior of systems provided with nonlinear dynamic vibration absorbers.
17. R. S. Haxton and A. D. S. Barr 1972 *ASME Journal of Engineering for Industry* **94**, 119–125. The autoparametric vibration absorber.
18. J. B. Hunt and J.-C. Nissen 1982 *Journal of Sound and Vibration* **83**, 573–578. The broadband dynamic vibration absorber.
19. J.-C. Nissen, K. Popp and B. Schmalhorst 1985 *Journal of Sound and Vibration* **99**, 149–154. Optimization of a non-linear dynamic vibration absorber.
20. H. J. Rice and J. R. McCraith 1987 *Journal of Sound and Vibration* **116**, 545–559. Practical non-linear vibration absorber design.
21. J. J. Thomsen 1996 *Journal of Sound and Vibration* **197**, 403–425. Vibration suppression using self-arranging mass: effects of adding restoring force.
22. J. J. Thomsen 1997 *Vibrations and Stability: Order and Chaos*, New York: McGraw-Hill.
23. B. Balachandran and Y.-Y. Li 1997 *Proceedings of the DETC'97 ASME Design Engineering Technical Conferences* DETC97/VIB-4091, *Sacremento*, CA, 1–6. A mechanical filter concept to suppress crane load oscillations.

24. A. H. NAYFEH and B. BALACHANDRAN 1995 *Applied Nonlinear Dynamics*: *Analytical, Computational, and Experimental Methods.* New York: Wiley.
25. R. J. RICHARDS 1979 *An Introduction to Dynamics & Control.* New York: Longman.
26. E. J. DOEDEL, X. J. WANG and T. F. FAIRGRIEVE 1994 *AUTO94: software for continuation and bifurcation problems in ordinary differential equations.* Concordia University, Montreal, Canada.